



1 **Soil infiltration characteristics and pore distribution under**
2 **freezing-thawing conditions**

3 **Ruiqi Jiang^{1,2,3,*}, Tianxiao Li^{1,2,3,*}, Dong Liu^{1,2,3,*}, Qiang Fu^{1,2,3,*}, Renjie Hou^{1,2,3},**
4 **Qinglin Li¹, Song Cui^{1,2,3}, Mo Li^{1,2,3}**

5 ¹ School of Water Conservancy & Civil Engineering, Northeast Agricultural University, Harbin 150030,
6 China

7 ² Key Laboratory of Effective Utilization of Agricultural Water Resources of Ministry of Agriculture,
8 Northeast Agricultural University, Harbin, Heilongjiang 150030, China

9 ³ Heilongjiang Provincial Key Laboratory of Water Resources and Water Conservancy Engineering in Cold
10 Region, Northeast Agricultural University, Harbin, Heilongjiang 150030, China

11 *** Dong Liu and Qiang Fu are corresponding authors.**

12 **★ These authors contributed equally to this work.**

13 *Corresponding author at: School of Water Conservancy and Civil Engineering, Northeast Agricultural
14 University, Harbin, Heilongjiang 150030, China

15 *Correspondence to:* liudong9599@yeah.net (Dong Liu). fuqiang0629@126.com (Qiang Fu)

16 **Abstract.** Frozen soil infiltration widely occurs in hydrological processes such as seasonal soil freezing and
17 thawing, snowmelt infiltration, and runoff. Accurate measurement and simulation of parameters related to
18 frozen soil infiltration processes are highly important for agricultural water management, environmental
19 issues and engineering problems in cold regions. Temperature changes cause soil pore size distribution
20 variations and consequently dynamic infiltration capacity changes during different freeze-thaw periods. To
21 better understand these complex processes and to reveal the freeze-thaw action effects on soil pore



23 distribution and infiltration capacity, selected black and meadow soils and chernozem, which account for the
24 largest arable land area in Heilongjiang Province, China. Laboratory tests of soils at different temperatures
25 were conducted using a tension infiltrometer and ethylene glycol aqueous solution. The stable infiltration
26 rate, hydraulic conductivity were measured, and the soil pore distribution was calculated. The results
27 indicated that for the different soil types, macropores, which constituted approximately 0.1% to 0.2% of the
28 soil volume under unfrozen conditions, contributed approximately 50% of the saturated flow, and after soil
29 freezing, the soil macropore proportion decreased to 0.05% to 0.1%, while their saturated flow proportion
30 decreased to approximately 30%. Soil moisture froze into ice crystals inside relatively large pores, resulting
31 in numerous smaller-sized pores, which reduced the number of macropores while increasing the number of
32 smaller-sized mesopores, so that the frozen soil infiltration capacity was no longer solely dependent on the
33 macropores. After the ice crystals had melted, more pores were formed within the soil, enhancing the soil
34 permeability.

35 **Key words:** Freezing-thawing soil; Hydraulic conductivity; Pore distribution; Macropores; Infiltration
36 characteristics

37 **1 Introduction**

38 Over the last few decades, the temperature changes caused by global warming have altered the freezing state
39 of near-surface soils, and in China, changes in characteristic values such as the mean annual area extent of
40 seasonal soil freeze/thaw state and maximum freezing depth indicate the degradation of frozen soil,
41 especially at high latitudes (Wang et al., 2019; Peng et al., 2016). Under the effect of temperature, most frozen
42 regions experience the seasonal freezing and thawing of soil, accompanied by coupled soil water and heat
43 movement and frost heave processes, thus making the soil structure and function more variable (Oztas and
44 Fayetorbay, 2003; Fu et al., 2019; Gao et al., 2018). Parameters such as the soil infiltration rate and hydraulic



45 conductivity are key factors in the study of soil water movement, groundwater recharge, and solute and
46 contaminant transport simulation (Angulo-Jaramillo et al., 2000). In regard to unfrozen soils, the temperature
47 has been shown to change the soil structure and kinematic viscosity of soil water, thereby affecting the
48 unsaturated hydraulic conductivity of soils (Gao and Shao, 2015). In terms of frozen soils, the water
49 infiltration characteristics and pore size distribution are highly variable and difficult to observe (Watanabe
50 et al., 2013); moreover, the water movement in freezing-thawing soils is complicated by the migration of
51 water and heat and the associated water phase change (Jarvis et al., 2016). The accurate measurement of
52 water movement parameters and soil pore distribution under freeze-thaw conditions is a necessary
53 prerequisite for the quantitative description of the water movement in frozen soil, and the mechanism and
54 degree of influence of the temperature on the infiltration rate, hydraulic conductivity, porosity and other
55 parameters in the different stages of freeze-thaw periods require further research.

56 Currently, the studies related to the quantitative characterization of freezing-thawing soil infiltration can be
57 mainly divided into experimental and model studies. Field experiments have been performed less often
58 because under natural conditions, the infiltration water establishes a preferential flow into the deep soil, and
59 the alternating freeze-thaw effect forms ice crystals to block the flow path through large pores, subsequently
60 limiting water infiltration (Daniel et al., 1997), while the melting effect of the infiltration water on ice makes
61 it difficult to reach a steady infiltration state. Controlled laboratory experiments provide new opportunities
62 for the simulation of frozen soil infiltration processes and the measurement of infiltration parameters.
63 Williams and Burt (1974) conducted early direct measurements in the laboratory, resolved the water freezing
64 problem by adding lactose and applied dialysis membranes on both sides of soil columns, and they
65 determined the water conductivity of saturated specimens in the horizontal direction (Burt and Williams,
66 1976). Andersland et al. (1996) measured the hydraulic conductivity of frozen granular soils at different



67 saturations using a conventional drop permeameter with decane as the permeant and concluded that the
68 hydraulic conductivity was the same as that of unfrozen soils with water as the infiltration solution.
69 McCauley et al. (2002) determined and compared the differences in hydraulic conductivity, permeability and
70 infiltration rate between frozen and unfrozen soils using diesel mixtures as permeants, and their results
71 indicated that the ice content determines whether soil is sufficiently impermeable. Zhao et al. (2013)
72 quantified the unsaturated hydraulic conductivity of frozen soil using antifreeze instead of water, adopted a
73 multistage outflow method under controlled pressures and introduced the pore impedance coefficient.
74 However, most of these studies did not consider the differences in kinematic viscosity and surface tension
75 between soil water and other solutions, which often results in hydraulic conductivity estimation, and the
76 homemade devices in the laboratory are often inconvenient for generalization in the field. Due to the dynamic
77 changes in the temperature and moisture phase, direct measurement is difficult, and hydraulic conductivity
78 empirical equations and models of frozen soil have been developed. First, the frozen soil hydraulic
79 conductivity was simply considered to follow a power exponential relationship with the temperature (Nixon,
80 1991;Smith, 1985), while others considered the hydraulic conductivity of frozen soil to be equal to that of
81 unfrozen soil at the same water content and assumed that the hydraulic conductivity of frozen soil was a
82 function of the moisture content of unfrozen soil (Lundin, 1990;Flerchinger and Saxton, 1989;Harlan, 1973).
83 On the basis of Campbell's model (Campbell, 1985), Tarnawski and Wagner (1996) proposed a frozen soil
84 hydraulic conductivity model based on the soil particle size distribution and porosity. Watanabe and Wake
85 (2008) viewed soil pores as cylindrical capillaries and suggested that ice formation occurs at the center of
86 these capillaries and established a model to describe the movement of thin film water and capillary water in
87 frozen soil based on the theory of capillaries and surface absorption (Watanabe and Flury, 2008). The
88 similarity between freezing and soil moisture profiles has been demonstrated (Spaans and Baker,



89 1996;Spaans, 1994), and subsequently, freezing profiles have been applied to estimate the unsaturated
90 hydraulic conductivity of frozen soils (Azmatch et al., 2012), which has been combined with field tests and
91 inversion models to achieve a high accuracy (Cheng et al., 2019).

92 Understanding the distribution characteristics of the soil pore system is essential for the evaluation of the
93 water and heat movement processes in soil. The soil macroporosity has been shown to impose a major impact
94 on water cycle processes such as infiltration, nutrient movement and surface runoff. (Demand et al.,
95 2019;Jarvis, 2007). The macroporosity is widespread in a variety of soils and produces preferential flow in
96 both frozen and unfrozen soils (Mohammed et al., 2018;Beven and Germann, 2013), and the prefreeze
97 moisture conditions affect the amount and state of ice in the macropores of frozen soils, resulting in a notable
98 variability in the infiltration capacity of thawed soils (Hayashi et al., 2003;Granger et al., 1984). Field
99 experiments on frozen soil have also demonstrated that macropores accelerate the infiltration rate (Stähli et
100 al., 2004;Kamp et al., 2003), the number and size of macropores affect the freezing and infiltration capacity
101 of soil layers to different extents, and low temperatures cause infiltration water to refreeze inside macropores
102 (Watanabe and Kugisaki, 2017;Stadler et al., 2000). Research on the frozen soil macroporosity has largely
103 focused on the qualitative analysis of its impact on the soil structure and infiltration capacity, and with the
104 development of experimental techniques, certain new methods and techniques, such as computed
105 tomography (CT) and X-ray scanning, have been applied to measure the number and distribution of
106 macropores (Taina et al., 2013;Bodhinayake et al., 2004;Grevers et al., 1989), but the lack of sampling
107 techniques targeting frozen soil still restricts related research.

108 Many limitations and deficiencies remain in the direct measurement of frozen soil infiltration characteristics
109 and pore distribution, and the relevant models also require a large amount of measured data to meet the
110 accuracy and applicability requirements. In this paper, the stable infiltration rate and hydraulic conductivity



111 of three types of soils at different temperatures were measured by precise control of the soil and ambient
112 temperatures, and the macropore and mesopore size distribution was calculated by using a tension
113 infiltrometer and a glycol aqueous solution as the infiltration medium. The conclusions provide a basis and
114 reference for the numerical simulation of the coupled water-heat migration process of freezing-thawing soil
115 and related parameterization studies.

116 **2 Materials and methods**

117 **2.1 Test plan**

118 Referring to arable land area data of various regions of Heilongjiang Province, the three types of soils that
119 dominate the cultivated land area in Heilongjiang Province are black and meadow soils and chernozem
120 (Bureau, 1992). Harbin, Zhaoyuan and Zhaozhou were selected as typical soil areas for sampling. A 5-cm
121 surface layer of floating soil and leaves was removed, and topsoil samples were collected at depths ranging
122 from 0-20 cm. After natural air drying and artificial crushing, the soil was sieved, and particles larger than 2
123 mm in diameter were removed. The remainder was used to prepare soil columns. The basic physical and
124 chemical parameters of the test soils, such as the bulk density, organic content and mechanical parameters,
125 are listed in Table 1.

126 **Table 1**

127 **Basic physical and chemical properties of three kind of soils**

Soil types	Bulk density (g/cm ³)	Organic content (g/kg)	Electrical conductivity (s/m)	Particle size (sand-silt-clay) (%)	Soil texture
Black soil	1.31	28.32	0.02	12.64-70.82- 16.54	silt loam



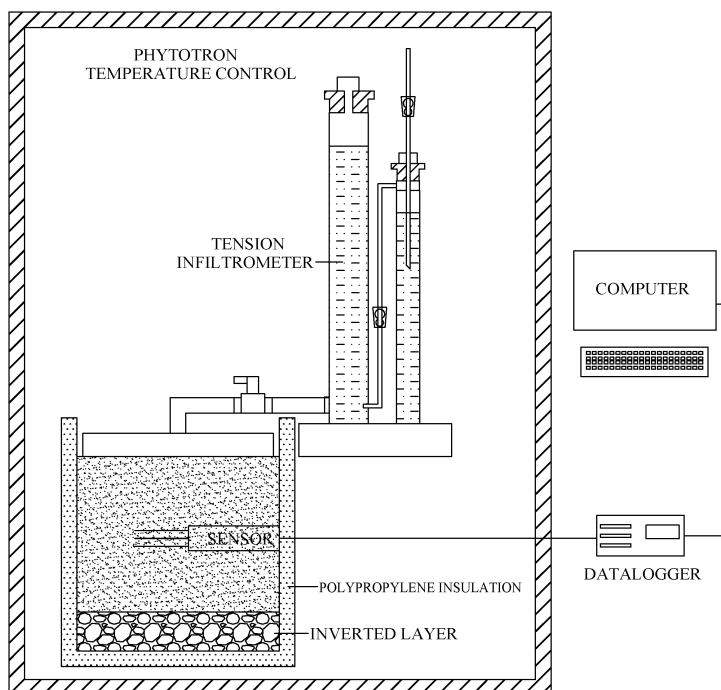
Meadow	1.22	16.51	0.01	9.52-73.00-17.48
soil				
Chernozem	1.15	26.52	0.01	38.99-50.30- 10.71

128 An artificial climate chamber was applied to control the temperature of the soil column and infiltration
129 solution, and four temperature treatments were established with three replications for each treatment: 15°C,
130 unfrozen soil, representing the soil before freezing, which was recorded as 15°C (BF); -5°C, stable freezing;
131 -10°C, stable freezing; and freezing at -10°C followed by thawing at 15°C, representing the soil after melting,
132 which was recorded as 15°C (AM). The freezing and thawing times were both 48 h. When the soil
133 temperature was consistent with the set temperature in the climate chamber, the samples were considered to
134 be completely frozen, and the effect of the number of freezing and thawing cycles was not considered in this
135 test. According to the basic information of the original soil, the volumetric moisture content of the sieved
136 soil was 30%, with a dry bulk density of 1.2 g/cm³. To ensure a homogeneous column, the soil was loaded
137 into a polyvinyl chloride (PVC) cylinder at 5-cm depth intervals, and petroleum jelly was applied to the sides
138 to reduce the sidewall flow (Lewis and Sjöström, 2010). The PVC cylinder was 26 cm in diameter and 30
139 cm in height, with a perforated plate at the bottom. To prevent lateral seepage, the barrel occurred 5 cm
140 above the soil surface, and the thickness of the soil layer was 20 cm. A HYDRA-PROBE II sensor
141 (STEVENS Water Monitoring Systems, Inc., Portland, Oregon, USA) was inserted in the middle of the pail
142 to observe the potential soil temperature and liquid water content change to determine whether ice melting
143 occurred. A 5-cm thick layer of sand and gravel was emplaced below the soil column, and a 5-cm thick layer
144 of black polypropylene insulation cotton was wrapped around the outer layer and bottom of the soil column.
145 The stable infiltration rate under tension levels of -3, -5, -7, -9, -11, and -13 cm was measured with a tension



146 infiltrometer, and the infiltration time and cumulative infiltration were recorded. The detailed layout of the
147 test apparatus is shown in Fig. 1.

148 The addition of a certain amount of lactose, antifreeze or other substances to water greatly reduces the
149 freezing point of water (Zhao et al., 2013; Williams and Burt, 1974) so that the soil macropores are not
150 quickly filled with ice with decreasing temperature, thereby maintaining better conditions for water flow. To
151 further verify the feasibility of the use of deionized water to prepare an aqueous solution of ethylene glycol
152 at a mass concentration of 40% as the infiltration medium for the frozen soil measurements, the surface
153 tension of the aqueous glycol solution at -5°C and -10°C and its relationship with the temperature were
154 measured with a contact angle measuring instrument (OCA20, DataPhysics Instruments, Germany) and a
155 surface tension measuring instrument (DCAT-21, DataPhysics Instruments, Germany), respectively. As an
156 example, the contact angle measurement process of the black soil at -10°C with the aqueous ethylene glycol
157 solution is shown in Fig. 2, and it is observed that the contact angle decreases to 0° within a few seconds
158 after the liquid droplet is placed on the soil, and the liquid droplet completely dissolves in the frozen soil,
159 which implies that the addition of glycol to water does not alter the wetting ability of the soil particles (Lu
160 and Likos, 2004). The relevant physicochemical properties of the aqueous ethylene glycol solution and water
161 are compared in Table 2.



162

163

Fig. 1. Diagram of the test equipment.



164

165 Fig. 2. Process of the contact angle measurement between the aqueous ethylene glycol solution and black
 166 soil at -10°C.

167

Table 2

168

Comparison of the physicochemical properties of the 40% ethylene glycol aqueous solution and

169

water

Infiltration solution	Temperature (°C)	Density (g/cm ³)	Dynamic viscosity (mPa.s)	Surface tension (mN/m)	Contact angle (°)
-----------------------	---------------------	---------------------------------	------------------------------	---------------------------	----------------------



Water	15	0.9991	1.14	73.56	0
Ethylene glycol	-5	1.0683	7.18	48.89	0
aqueous solution	-10	1.0696	9.06	49.10	0

170 **2.2 Measurement of the frozen soil hydraulic conductivity**

171 Gardner (1958) proposed that the unsaturated hydraulic conductivity of soil varies with the matric
 172 potential:

173
$$K(h) = K_{sat} \exp(\alpha h) \quad (1)$$

174 where K_{sat} is the saturated hydraulic conductivity, cm/hour, and h is the matric potential or tension, cm H_2O .

175 Wooding (1968) considered that the steady-state unconfined infiltration rate into soil from a circular water
 176 source of radius R can be calculated with the following equation:

177
$$Q = \pi R^2 K \left[1 + \frac{4}{\pi R \alpha} \right] \quad (2)$$

178 where Q is the amount of water entering the soil per unit time, cm^3/h ; K is the hydraulic conductivity,
 179 $cm/hour$; and α is a constant. Ankeny et al. (1991) proposed that implementing two successively applied
 180 pressure heads h_1 and h_2 could yield the unsaturated hydraulic conductivity, and upon replacing K in Eq. (2)
 181 with Eq. (1), the following is obtained:

182
$$Q_1(h) = \pi R^2 K_{sat} \exp(\alpha h) \left[1 + \frac{4}{\pi R \alpha} \right] \quad (3)$$

183
$$Q_2(h) = \pi R^2 K_{sat} \exp(\alpha h) \left[1 + \frac{4}{\pi R \alpha} \right] \quad (4)$$

184 Dividing Eq. (4) by Eq. (3) and solving for α yields:

185
$$\alpha = \frac{\ln[Q(h_2)/Q(h_1)]}{h_2 - h_1} \quad (5)$$

186 where $Q(h_1)$ and $Q(h_2)$ can be measured, h_1 and h_2 are the preset tension values, and α can be calculated with



187 Eq. (5). The result can be substituted into Eq. (3) or (4) to calculate K_{sat} . When the number of tension levels
188 is larger than 2, parameter fitting methods can be applied to improve the accuracy of α and K_{sat} (Hussen and
189 Warrick, 1993).

190 The tension is controlled by the bubble collecting tube of the tension infiltrometer, and different pressure
191 heads h correspond to different pore sizes r . By applying different pressure heads h to the soil surface, water
192 will overcome the surface tension in the corresponding pores and be discharged, and the infiltration volume
193 is recorded after reaching the stable infiltration state.

194 Under the assumption that the frozen soil pore ice pressure is equal to the atmospheric pressure and that
195 solutes are negligible, the Clausius-Clapeyron equation can be adopted to achieve the interconversion
196 between the soil temperature and suction (Konrad and Morgenstern, 1980; Watanabe et al., 2013), which can
197 be simplified as follows:

$$198 \quad \psi = -L\rho_w \frac{T}{273.15} \quad (6)$$

199 where ψ is the soil suction, kPa; L is the latent heat of fusion of water, 3.34×10^5 J/kg; ρ_w is the density of
200 water, 1 g/cm^3 ; and T is the subfreezing temperature, °C. After the unit conversion of the soil suction into h
201 (cm H_2O), the unsaturated hydraulic conductivity of frozen soil at different negative temperatures can be
202 obtained via substitution into Eq. (2).

203 **2.3 Measurement of the pore size distribution in frozen soil**

204 As a nonuniform medium, soil consists of pores of various pore sizes, and the equation for the soil pore
205 radius r can be obtained from the capillary model (Watson and Luxmoore, 1986):

$$206 \quad r = - \frac{2\sigma \cos \beta}{\rho g h} \quad (7)$$

207 where σ is the surface tension of the solution, g/s^2 ; β is the contact angle between the solution and pore wall;



208 ρ is the density of the solution, g/cm^3 ; g is the acceleration of gravity, m/s^2 ; and h is the corresponding tension
209 of the tension infiltrometer, $\text{cm H}_2\text{O}$.

210 The effective macroporosity θ_m can be calculated for various soil particle sizes based on the Poiseuille
211 equation (Wilson and Luxmoore, 1988):

$$212 \quad \theta_m = 8\mu K_m / \rho g r^2 \quad (8)$$

213 where μ is the dynamic viscosity of the fluid, $\text{g/(cm}^2\text{s)}$; K_m is the macropore hydraulic conductivity and is
214 defined as the difference between $K(h)$ at various tension gradients, cm/h ; and r is the corresponding
215 equivalent pore size. The effective porosity is equal to the number of pores per unit area multiplied by the
216 area of the corresponding pore size. For different pore sizes, the maximum number of effective macropores
217 per unit area N can be calculated with the following equation:

$$218 \quad N = \theta_m / \pi r^2 \quad (9)$$

219 where N is the number of effective macropores per unit area, and Eq. (7) calculates the minimum value of
220 the pore radius, while the result obtained with Eq. (9) is actually the maximum number of effective
221 macropores per unit area and the maximum porosity.

222 Considering the differences in surface tension and density between the aqueous ethylene glycol solution and
223 water, when calculating the frozen soil pore size distribution, it is necessary to convert the tension into the
224 equivalent pore radius according to Eq. (7), which is classified and subdivided into large and medium pores
225 according to the common classification method (Luxmoore, 1981), the details of which are listed in Table 3,
226 while the corresponding tension values in Table 3 are substituted into the fitting curve equation to calculate
227 the corresponding stable infiltration rate q and unsaturated hydraulic conductivity K .

228 **Table 3**

229 **Tension and equivalent pore radius conversions**

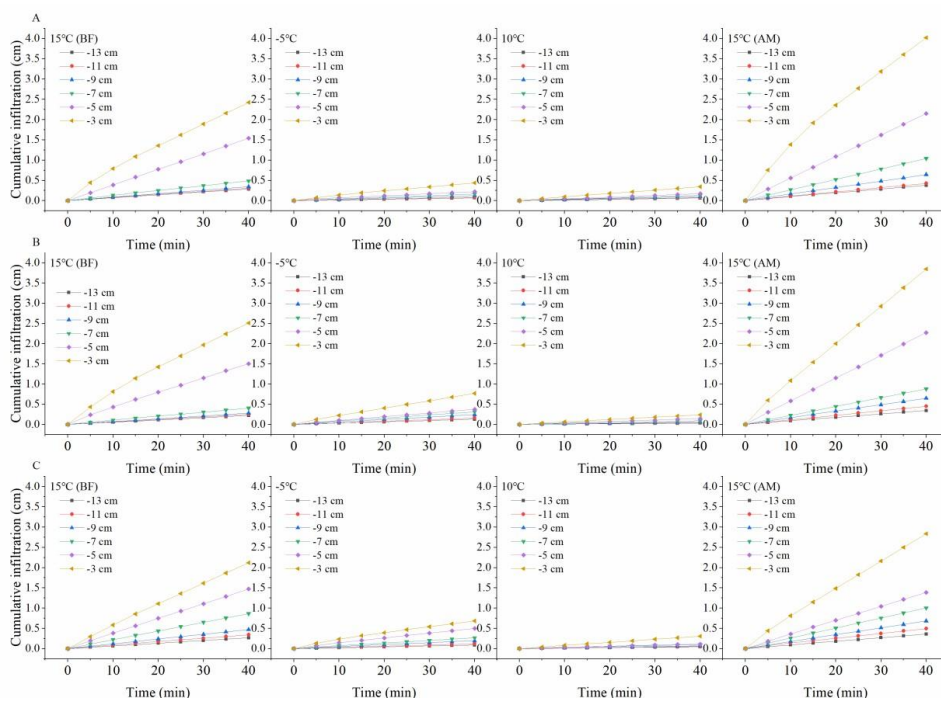


Pore types	Pore radius (mm)	Tension conversion (cm)		
		Water (15°C)	Ethylene glycol aqueous solution (- 5°C)	Ethylene glycol aqueous solution (- 10°C)
Macroporous	>0.5	0~3	0~1.86	0~1.87
	0.3-0.5	3~5	1.86 ~3.11	1.86 ~3.12
Mesoporous	0.15-0.3	5~10	3.11~6.22	3.12~6.23
	0.1-0.15	10~15	6.22~9.32	6.23~9.35
	0.05-0.1	15~30	9.32~18.65	9.35~18.70

230 **3 Results**

231 **3.1 Infiltration characteristics of freezing-thawing soils**

232 According to the recorded cumulative infiltration and duration, curves of the cumulative infiltration and
 233 infiltration rate were plotted over time, as shown in Figs. 3 and 4, respectively. The constant α and saturated
 234 hydraulic conductivity K_{sat} were calculated under different tensions h and corresponding steady-state
 235 infiltration rates q , and the unsaturated hydraulic conductivity under different tensions was calculated with
 236 Eq. (1). The stable infiltration rate and unsaturated hydraulic conductivity at different temperatures are
 237 shown in Fig. 5, and the details of α and K_{sat} are listed in Table 4.

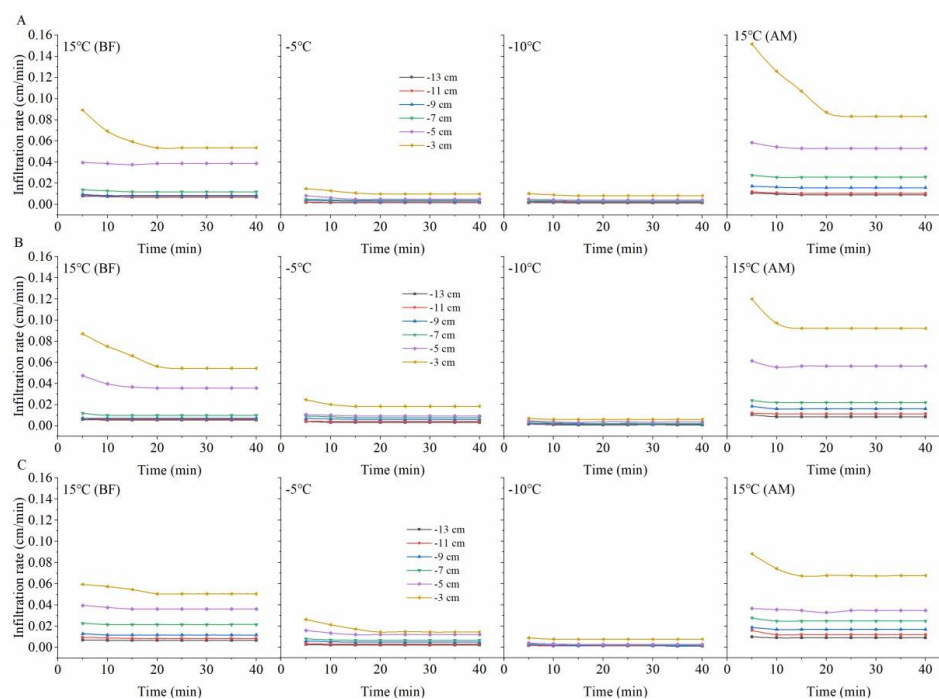


238

239 **Fig. 3.** Cumulative infiltration over time under the different treatments.

240 Note: A Black Soil; B Meadow Soil; C Chernozem.

241



242

243 **Fig. 4.** Infiltration rate over time under the different treatments.

244 Note: A Black Soil; B Meadow Soil; C Chernozem.

245 As shown in Figs. 4 and 5, under the different tension conditions, the infiltration capacity of the unfrozen
246 soil is basically consistent with the findings of field experiments and is highly influenced by the tension
247 value (Wang et al., 1998). Compared to the room-temperature soil, the cumulative infiltration of frozen soil
248 slowly increases, and the infiltration rate always remains low, while under the same negative temperature
249 treatment, the influence of the tension value is also greatly reduced. When the temperature was reduced to
250 10°C, few major tension differences were observed except for the maximum tension of -3 cm. From the
251 change in the slope of the two curves, we find that the time for the unfrozen soil to reach the stable infiltration
252 rate usually ranges from 15~20 min, while the time for the frozen soil to reach the stable infiltration rate is
253 usually 10 min under higher tensions of -3 and -5 cm and 5 min under lower tensions. Comparing the
254 infiltration process before and after the freezing and thawing of the soil, overall, the cumulative infiltration



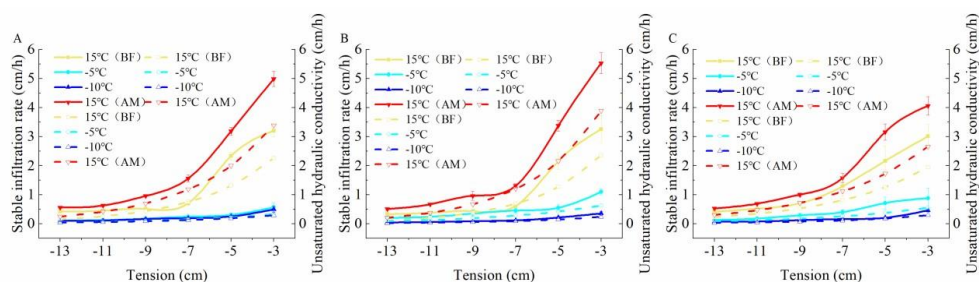
255 and infiltration rate exhibited varying degrees of increase with increasing tension value, and the increase
 256 amplitude expanded. Moreover, the difference in the cumulative infiltration and infiltration rate between the
 257 low tension levels ranging from -9 to -13 cm after soil thawing was larger than that before soil freezing,
 258 which also indirectly demonstrated that freezing and thawing could further stabilize the soil pore distribution
 259 by affecting the homogeneity, which will be detailed in subsequent sections.

260 **Table 4**

261 **Infiltration parameters of the different temperature treatments of the three soil types**

Soil types	Temperature (°C)	α (cm/h)	K_{sat} (cm/h)
Black soil	15 (BF)	0.2742	5.1480
	-5	0.1993	0.5960
	-10	0.2028	0.5221
<hr/>			
Meadow soil	15 (AM)	0.2629	7.4658
	15 (BF)	0.3071	5.9232
	-5	0.1996	1.1385
Chernozem	-10	0.2477	0.4903
	15 (AM)	0.2934	9.3757
	15 (BF)	0.2166	3.7185
Chernozem	-5	0.1907	0.9739
	-10	0.2508	0.6077
	15 (AM)	0.2182	5.1283

262



263



264 **Fig. 5.** Variation curves of the unsaturated hydraulic conductivity and stable infiltration rate with the
265 tension for the different treatments of the three soils.

266 Note: A Black soil; B meadow soil; C chernozem. The solid lines represent the stable infiltration rate, and
267 the dashed lines represent the unsaturated hydraulic conductivity.

268 Combining Fig. 5 and Table 4, we observe that the three types of soils exhibit a high infiltration capacity
269 under normal temperature conditions. With increasing set tension value, the suction force of the soil matrix
270 gradually weakens, the constraint and maintenance capacity of the matric potential to the soil water decreases,
271 the number of pores involved in the soil water infiltration process increases, and the unsaturated hydraulic
272 conductivity and stable infiltration rate of the three types of soils all reveal different degrees of increase.

273 When the temperature was lowered from 15°C to -5°C and the soil reached the stable frozen state, the
274 saturated water conductivity of the black soil, meadow soil and chernozem soil decreased by 88.42%, 80.78%
275 and 73.8%, respectively. With decreasing soil temperature to -10 °C, due to the presence of liquid water in
276 the pores, the saturated water conductivity still exhibited a certain decrease over the prefreeze conditions
277 and continued to decrease by 1.43%, 10.94% and 9.85%, respectively. At negative temperatures, the
278 unsaturated hydraulic conductivity decreased considerably and fluctuated within a small range, mainly
279 because the unfrozen and saturated water contents were low after soil freezing. Comparing the two
280 treatments of -5°C and -10°C, the unsaturated hydraulic conductivity (ANOVA, $P=0.72$, $F=0.14$) and stable
281 infiltration rate (ANOVA, $P=0.71$, $F=0.15$) of the black soil revealed almost no significant change, indicating
282 that most of its pores were filled with ice crystals at -5°C and were no longer involved in water infiltration.

283 The unsaturated water conductivity of the meadow and chernozem soils still exhibited a more significant
284 reduction when the freezing temperature was further reduced to -10°C. When the temperature was raised
285 again to 15°C and the soil was completely thawed, the steady infiltration rate and saturated hydraulic

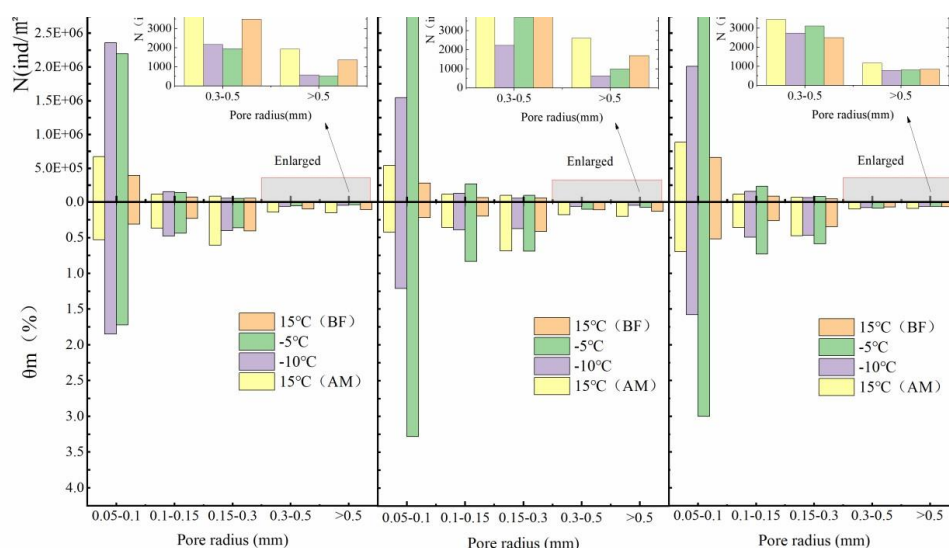


286 conductivity increased with increasing temperature, and the values were higher than those of the soil at the
 287 same temperature before freezing. The saturated hydraulic conductivity of the black soil, meadow soil and
 288 chernozem increased by 45.02%, 58.63% and 37.91%, respectively, over the 15°C (BF) treatment values.

289 3.2 Pore distribution characteristics of the freezing-thawing soil

290 Considering the differences in the physical and chemical properties between the infiltration solutions,
 291 infiltration parameters such as the hydraulic conductivity and stable infiltration rate alone do not fully reflect
 292 the infiltration characteristics and internal pore size of frozen soils. According to Eqs. (7)-(9), the maximum
 293 number per unit area N , effective porosity θ_m and percentage of pore flow to saturated flow P corresponding
 294 to the different soil pore sizes of the three soils under the different temperature treatments are calculated, as
 295 shown in Figs. 6 and 7.

296

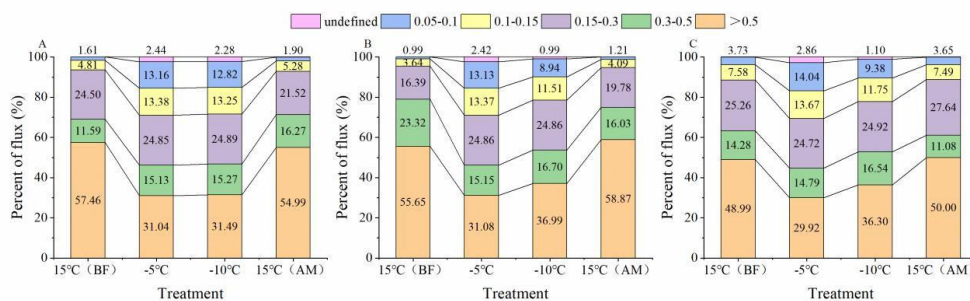


297

298 **Fig.6.** Number of pores and effective porosity of the different equivalent pores.



299 Note: A Black Soil; B Meadow Soil; C Chernozem.



300

301 **Fig. 7.** Percentage of the pore flow in the saturated flow for the different equivalent pore sizes.

302 Note: A Black Soil; B Meadow Soil; C Chernozem.

303 Fig. 6 shows that pores of different equivalent radii widely occur in all three soils, and under all four
 304 temperature treatments, the largest N value is that for the medium pores with an equivalent radius of 0.05-
 305 0.1 mm, and N gradually decreases with increasing equivalent radius size. Under the two room-temperature
 306 treatments at 15°C (BF) and 15°C (AM), the largest number of 0.05- to 0.1-mm medium pores and the
 307 smallest number of >0.5-mm macropores differed by two orders of magnitude, and the number of pores of
 308 each size exhibited different degrees of increase or decrease over the two treatments at -5°C and -10°C where
 309 freezing occurred, with the number of medium pores with an equivalent pore size of 0.05-0.1 mm
 310 significantly changing. Increases of more than an order of magnitude were achieved in all three soils, while
 311 the macropores with an equivalent pore size of >0.5 mm were generally reduced by an order of magnitude,
 312 with the difference in the number of pores of these two sizes reaching four orders of magnitude. This
 313 indicates that freezing caused by temperature change significantly alters the soil internal structure, with ice
 314 crystals forming in the relatively large pores containing the internal soil moisture, resulting in a large number
 315 of smaller pores. Assessing the two treatments at -5°C and -10°C separately, when the temperature was
 316 lowered from -5°C to -10°C, the number of pores in each pore size interval of the meadow and chernozem



317 soils exhibited a significant decrease, while the black soil revealed a small increase, which might be related
318 to the high organic matter content of the black soil. Comparing the two treatments at 15°C (BF) and 15°C
319 (AM), the number of pores in all three soils increased to different degrees after thawing, and more pores
320 were formed with the melting of ice crystals after freeze-thaw destruction of the soil particles, which
321 enhanced the soil water conductivity.

322 Comprehensive analysis of Figs. 6 and 7 reveals that before freezing, the θ_m of the various pore sizes of the
323 black and meadow soils and chernozem with an equivalent radius of >0.5 mm were 0.11%, 0.13% and 0.07%,
324 respectively, while the P value reached 57.46%, 55.65% and 48.99%, respectively, with the values of the
325 thawed soil similar to these values. This indicates that for all five soil pore sizes under unfrozen conditions,
326 although the number of macropores with a pore size >0.5 mm is the smallest and the effective porosity is the
327 lowest, their contribution to the saturated flow is usually more than half, and the macropores need only
328 represent a small fraction of the pore volume to significantly contribute to the soil water flow. For the frozen
329 soil, the P value of the >0.5 -mm macropores was significantly reduced and remained at approximately 30%
330 after the reduction, while the P value of the smaller pore sizes such as 0.15-0.3 mm, 0.1-0.15 mm, and 0.05-
331 0.1 mm, revealed different degrees of increase. Moreover, the smaller the pore size was, the greater the P
332 value increased, and their contribution eventually accounted for more than 10% of the saturated flow. The
333 saturated flow became more evenly distributed across the pores of each size, and the total proportion of
334 medium pores exceeded that of the macropores. This indicates that the freezing action caused obvious
335 changes to the soil structure, pore size and quantity, and although the macropores still played an important
336 role, the infiltration capacity of the frozen soil no longer relied solely on these macropores, and the
337 contribution of certain smaller-sized mesopores to the infiltration capacity of the frozen soil could no longer
338 be neglected. Selecting the black soil as an example, the total effective porosity of the pores of each size



339 under the four treatments was 1.15%, 2.62%, 2.84%, and 1.80%, and the P values were 99.97%, 97.56%,
340 97.72%, and 99.96%, respectively, which implies that the soil water infiltrated almost entirely via the large
341 and medium pores. The small micropores, even in large numbers, contributed little to the infiltration process.

342 **4 Discussion**

343 **4.1 Permeability and hydraulic conductivity of the frozen soil**

344 In the field environment, although it is difficult to accurately measure the infiltration rate of frozen soils
345 using traditional instruments and methods such as single-loop infiltrators, the obtained test results still
346 demonstrate that the infiltration capacity decreases by one or more orders of magnitude when the soil is
347 frozen (Stähli et al., 2004). Although the cumulative infiltration and infiltration rate of frozen soil are low,
348 the presence of unfrozen water allows a certain amount of infiltration flow to be maintained in the soil. When
349 water is applied as the infiltration solution, the low temperature in the frozen soil easily causes the infiltration
350 water to freeze, thus forming a thin layer of ice on the soil particle surface and delaying the subsequent
351 infiltration of water. This phenomenon results in a low infiltration rate after the freezing of soils with a high
352 initial water content and a relatively high infiltration rate after the freezing of dry soils (Watanabe et al.,
353 2013), because the higher the ice content is, the more latent heat needs to be overcome to melt any ice crystals,
354 resulting in a weakened propagation of the melting front, thus limiting the infiltration rate so that it is
355 controlled by the downward movement of the melting leading edge of the ice crystals (Pittman et al., 2020).
356 During the measurements using the tension infiltrator in this study, the sensor temperature always remained
357 consistent with the soil temperature, indicating that the use of an aqueous glycol solution could be a useful
358 way to avoid the problem of freezing of the infiltration solution. In addition, the hydraulic conductivity of
359 frozen soils with different capacities and at various water flow rates was demonstrated not to greatly differ
360 (Watanabe and Osada, 2017).



361 Whether water or other low-freezing point solutions are applied as infiltration media, the hydraulic
362 conductivity of frozen soil significantly changes only within a limited temperature range above -0.5°C
363 depending on the unfrozen water and ice contents, and at a soil temperature below -0.5°C , the hydraulic
364 conductivity usually decreases to below 10^{-10} m/s (Watanabe and Osada, 2017; Williams and Burt, 1974).
365 The unsaturated hydraulic conductivity in our experiments was measured at a set tension level, and according
366 to Eq. (6), the soil substrate potential increases by 125 m for every 1°C decrease in temperature (Williams
367 and Smith, 1989), while the frozen soil hydraulic conductivity calculated at -5°C and -10°C , which
368 corresponds to the actual matric potential, is much lower than 10^{-10} m/s and can be ignored. This suggests
369 that even under ideal conditions where no heat exchange occurs between the infiltration solution and the soil
370 and no freezing of the infiltration water takes place to prevent the subsequent infiltration, the unsaturated
371 hydraulic conductivity of the frozen soil is so low that the frozen soil at lower temperatures in its natural
372 state could be considered impermeable, both for water and other solutions.

373 **4.2 Effect of the freeze-thaw cycles on soil pore distribution**

374 In our study, the N value after freezing for the different types of soil was approximately 1000-2000/m² using
375 the tension infiltrator, which agreed well with other studies and remained at a same magnitude (Pittman et
376 al., 2020), indicating that the method is generally reliable. The freeze-thaw effect significantly improves the
377 water conductivity of the different types of soils because it increases the porosity, decreases the soil
378 compactness and dry weight, and thus increases the soil water conductivity (Fouli et al., 2013). On this basis,
379 we also found that the freeze/thaw process significantly alters the size and number of soil pores, especially
380 after freezing, and the number of macropores decreases, while the contribution of macropores to the saturated
381 flow decreases. The proportion of the saturated flow in the mesopores with a pore size of <0.3 mm
382 approaches or even exceeds the proportion in the macropores, indicating that the soil water inside relatively



383 large pores is more likely to freeze, which in turn creates a large number of small pores, whereas the water
384 transfer process in unfrozen soils primarily relies on the macropores, with obvious differences (Wilson and
385 Luxmoore, 1988; Watson and Luxmoore, 1986). The unsaturated water conductivity of the frozen soils
386 measured in this study is quite low, but under human control (Watanabe and Kugisaki, 2017) or natural
387 conditions in the field (Espeby, 1990), water has been shown to infiltrate into frozen soils through
388 macropores as long as the pore size is large enough. Considering that the soil in this experiment is disturbed
389 soil that has been air dried and sieved, although the macropores created by tillage practices (Lipiec et al.,
390 2006) and invertebrate activities (Lavelle et al., 2006) are excluded, due to the inherent heterogeneity of the
391 soil particles, macropores remain in the uniformly filled soil column (Cortis and Berkowitz, 2004; Oswald et
392 al., 1997), and these macroporous pores still play a role in determining the infiltration water flow.

393 Studies related to the frozen soil macropore flow and pore distribution are still quite few and more data
394 should be acquired and more models should be developed to better understand the water movement in frozen
395 soil regions. In subsequent studies, we will consider applying the methods used in this paper to field
396 experiments to examine the dynamics of the infiltration capacity and pore distribution in nonhomogeneous
397 soils during whole freeze-thaw periods under real outdoor climatic conditions, such as lower temperatures
398 and more severe freeze-thaw cycles, but the infiltration solution must be carefully selected, as ethylene glycol
399 is toxic, to prevent contamination of agricultural soils and crops, and a certain concentration of lactose could
400 be considered (Burt and Williams, 1976; Williams and Burt, 1974). Measurements should focus on frozen
401 soil layers at different depths, especially in the vicinity of freezing peaks, and the spatial variability in the
402 distribution of frozen soil pores should be investigated. This work helps to improve the accuracy of
403 simulations such as those of frozen soil water and heat movement or snowmelt water infiltration processes.

404 **5 Conclusions**



405 In this paper, the infiltration capacity of soil columns under four temperature treatments representing various
406 freeze-thaw stages was measured, and the distribution of the pores of various sizes within the soil was
407 calculated based on the measurements by applying an aqueous ethylene glycol solution with a tension
408 infiltrator in the laboratory. The results revealed that for the three types of soils, i.e., black soil, meadow soil
409 and chernozem, the macropores, which accounted for only approximately 0.1% to 0.2% of the soil volume
410 at room temperature, contributed approximately 50% to the saturated flow, and after freezing, the proportion
411 of macropores decreased to 0.05% to 0.1%, while their share of the saturated flow decreased to
412 approximately 30%. Coupled with the even smaller mesopores, the large and medium pores, accounting for
413 approximately 1% to 2% of the soil volume, conducted almost all of the soil moisture under saturated
414 conditions. Freezing decreased the number of macropores and increased the number of smaller-sized
415 mesopores, thereby significantly increasing their contribution to the frozen soil infiltration capacity so that
416 the latter was no longer solely dependent on the macropores. The infiltration parameters and pore distribution
417 of the black soil were the least affected by the different negative freezing temperatures under the same
418 moisture content and weight capacity conditions, while those of the meadow soil were the most impacted.

419 **Data availability**

420 Data used in this study are available in the Figshare (doi: [10.6084/m9.figshare.12965123](https://doi.org/10.6084/m9.figshare.12965123)).

421 **Author contributions**

422 Ruiqi Jiang designed research program. Tianxiao Li and Ruiqi Jiang built and deployed the soil column and
423 instruments with assistance from Qinglin Li and Renjie Hou. Dong Liu and Qiang Fu provided funding for
424 test equipment. Song Cui collected soil samples in the field. Ruiqi Jiang and Tianxiao Li analyzed the
425 laboratory data. Ruiqi Jiang prepared the manuscript with comments from Tianxiao Li and Dong Liu.

426 **Competing interests**



427 The authors declare that they have no conflict of interest

428 **Acknowledgements**

429 We acknowledge that this research was supported by the National Natural Science Foundation of China
430 (51679039), the National Science Fund for Distinguished Young Scholars (51825901), the Heilongjiang
431 Provincial Science Fund for Distinguished Young Scholars (YQ2020E002), "Young Talents" Project of
432 Northeast Agricultural University (18QC28), China Postdoctoral Science Foundation Grant (2019M651247)

433 **References**

434 Andersland, O. B., Wiggert, D. C., and Davies, S. H.: Hydraulic conductivity of frozen granular soils, *J*
435 *Environ Eng*, 122, 212-216, 10.1061/(ASCE)0733-9372(1996)122:3(212), 1996.

436 Angulo-Jaramillo, R., Vandervaere, J.-P., Roulier, S., Thony, J.-L., Gaudet, J.-P., and Vauclin, M.: Field
437 measurement of soil surface hydraulic properties by disc and ring infiltrometers: A review and recent
438 developments, *Soil and Tillage Research*, 55, 1-29, 10.1016/S0167-1987(00)00098-2, 2000.

439 Ankeny, M. D., Ahmed, M., Kaspar, T. C., and Horton, R.: Simple field method for determining
440 unsaturated hydraulic conductivity, *Soil Sci Soc Am J*, 55, 467-470,
441 10.2136/sssaj1991.03615995005500020028x, 1991.

442 Azmatch, T. F., Sego, D. C., Arenson, L. U., and Biggar, K. W.: Using soil freezing characteristic curve to
443 estimate the hydraulic conductivity function of partially frozen soils, *Cold Reg. Sci. Technol*, 83, 103-109,
444 10.1016/j.coldregions.2012.07.002, 2012.

445 Beven, K., and Germann, P.: Macropores and water flow in soils revisited, *Water Resour Res*, 49, 3071-
446 3092, 10.1002/wrcr.20156, 2013.

447 Bodhinayake, W., Si, B. C., and Xiao, C.: New method for determining water - conducting macro - and
448 mesoporosity from tension infiltrometer, *Soil Sci Soc Am J*, 68, 760-769, 10.2136/sssaj2004.0760, 2004.

449 Bureau, H. L. A.: Heilongjiang soil, Agriculture Press, Beijing, 1992.



- 450 Burt, T., and Williams, P. J.: Hydraulic conductivity in frozen soils, *Earth Surface Processes*, 1, 349-360,
451 10.1002/esp.3290010404, 1976.
- 452 Campbell, G. S.: *Soil physics with BASIC: transport models for soil-plant systems*, Elsevier, Amsterdam,
453 1985.
- 454 Cheng, Q., Xu, Q., Cheng, X., Yu, S., Wang, Z., Sun, Y., Yan, X., and Jones, S. B.: In-situ estimation of
455 unsaturated hydraulic conductivity in freezing soil using improved field data and inverse numerical modeling,
456 *Agr Forest Meteorol*, 279, 107746, 10.1016/j.agrformet.2019.107746, 2019.
- 457 Cortis, A., and Berkowitz, B.: Anomalous transport in “classical” soil and sand columns, *Soil Sci Soc Am*
458 *J*, 68, 1539-1548, 10.2136/sssaj2004.1539, 2004.
- 459 Daniel, Stadler, and, Hannes, Flühler, and, Per-Erik, and Jansson: Modelling vertical and lateral water flow
460 in frozen and sloped forest soil plots, *Cold Regions Science & Technology*, 10.1016/S0165-232X(97)00017-7,
461 1997.
- 462 Demand, D., Selker, J. S., and Weiler, M.: Influences of macropores on infiltration into seasonally frozen
463 soil, *Vadose Zone J*, 18, 1-14, 10.2136/vzj2018.08.0147, 2019.
- 464 Espeby, B.: Tracing the origin of natural waters in a glacial till slope during snowmelt, *J Hydrol*, 118, 107-
465 127, 10.1016/0022-1694(90)90253-T, 1990.
- 466 Flerchinger, G. N., and Saxton, K. E.: *Simultaneous Heat and Water Model of a Freezing Snow-Residue-*
467 *Soil System I. Theory and Development*, American Society of Agricultural Engineers, 10.13031/2013.31041,
468 1989.
- 469 Fouli, Y., Cade-Menun, B. J., and Cutforth, H. W.: Freeze-thaw cycles and soil water content effects on
470 infiltration rate of three Saskatchewan soils, *Can J Soil Sci*, 93, 485-496, 10.4141/CJSS2012-060, 2013.
- 471 Fu, Q., Zhao, H., Li, T., Hou, R., Liu, D., Ji, Y., Zhou, Z., and Yang, L.: Effects of biochar addition on soil



- 472 hydraulic properties before and after freezing-thawing, *Catena*, 176, 112-124, 10.1016/j.catena.2019.01.008,
473 2019.
- 474 Gao, B., Yang, D., Qin, Y., Wang, Y., Li, H., Zhang, Y., and Zhang, T.: Change in frozen soils and its effect
475 on regional hydrology, upper Heihe basin, northeastern Qinghai-Tibetan Plateau, *Cryosphere*, 12, 657-673,
476 2018.
- 477 Gao, H., and Shao, M.: Effects of temperature changes on soil hydraulic properties, *Soil Till Res*, 153,
478 10.1016/j.still.2015.05.003, 2015.
- 479 Gardner, W.: Some steady-state solutions of the unsaturated moisture flow equation with application to
480 evaporation from a water table, *Soil Sci*, 85, 228-232, 10.1097/00010694-195804000-00006, 1958.
- 481 Granger, R. J., Gray, D. M., and Dyck, G. E.: Snowmelt infiltration to frozen Prairie soils, *Can J Earth Sci*,
482 21, 669-677, 10.1139/e84-073, 1984.
- 483 Grevers, M., JONG, E. D., and St. Arnaud, R.: The characterization of soil macroporosity with CT
484 scanning, *Can J Soil Sci*, 69, 629-637, 10.4141/cjss89-062, 1989.
- 485 Harlan, R.: Analysis of coupled heat - fluid transport in partially frozen soil, *Water Resour Res*, 9, 1314-
486 1323, 10.1029/WR009i005p01314, 1973.
- 487 Hayashi, M., Kamp, G. V.D., and Schmidt, R.: Focused infiltration of snowmelt water in partially frozen
488 soil under small depressions, *J Hydrol*, 270, 214-229, 10.1016/S0022-1694(02)00287-1, 2003.
- 489 Hussen, A., and Warrick, A.: Alternative analyses of hydraulic data from disc tension infiltrometers, *Water*
490 *Resour Res*, 29, 4103-4108, 10.1029/93WR02404, 1993.
- 491 Jarvis, N.: A review of non - equilibrium water flow and solute transport in soil macropores: Principles,
492 controlling factors and consequences for water quality, *Eur J Soil Sci*, 58, 523-546, 10.1111/j.1365-
493 2389.2007.00915.x, 2007.



- 494 Jarvis, N., Koestel, J., and Larsbo, M.: Understanding Preferential Flow in the Vadose Zone: Recent
495 Advances and Future Prospects, *Vadose Zone J*, 15, 10.2136/vzj2016.09.0075, 2016.
- 496 Kamp, G. v. d., Hayashi, M., and Gallén, D.: Comparing the hydrology of grassed and cultivated
497 catchments in the semi-arid Canadian prairies, *Hydrol Process*, 10.1002/hyp.1157, 2003.
- 498 Konrad, J.-M., and Morgenstern, N. R.: A mechanistic theory of ice lens formation in fine-grained soils,
499 *Can Geotech J*, 17, 473-486, 10.1139/t80-056, 1980.
- 500 Lavelle, P., Decaëns, T., Aubert, M., Barot, S. b., Blouin, M., Bureau, F., Margerie, P., Mora, P., and Rossi,
501 J.-P.: Soil invertebrates and ecosystem services, *Eur J Soil Biol*, 42, S3-S15, 10.1016/j.ejsobi.2006.10.002, 2006.
- 502 Lewis, J., and Sjöström, J.: Optimizing the experimental design of soil columns in saturated and
503 unsaturated transport experiments, *J Contam Hydrol*, 115, 1-13, 2010.
- 504 Lipiec, J., Kuś, J., Słowińska-Jurkiewicz, A., and Nosalewicz, A.: Soil porosity and water infiltration as
505 influenced by tillage methods, *Soil and Tillage research*, 89, 210-220, 10.1016/j.still.2005.07.012, 2006.
- 506 Lu, N., and Likos, W. J.: *Unsaturated soil mechanics*, Wiley, Hoboken, 2004.
- 507 Lundin, L.-C.: Hydraulic properties in an operational model of frozen soil, *J Hydrol*, 118, 289-310,
508 10.1016/0022-1694(90)90264-X, 1990.
- 509 Luxmoore, R.: Micro-, meso-, and macroporosity of soil, *Soil Sci Soc Am J*, 45, 671-672,
510 10.2136/sssaj1981.03615995004500030051x, 1981.
- 511 McCauley, C. A., White, D. M., Lilly, M. R., and Nyman, D. M.: A comparison of hydraulic conductivities,
512 permeabilities and infiltration rates in frozen and unfrozen soils, *Cold Reg. Sci. Technol*, 34, 117-125,
513 10.1016/S0165-232X(01)00064-7, 2002.
- 514 Mohammed, A. A., Kurylyk, B. L., Cey, E. E., and Hayashi, M.: Snowmelt infiltration and macropore flow
515 in frozen soils: Overview, knowledge gaps, and a conceptual framework, *Vadose Zone J*, 17, 1-15,



- 516 10.2136/vzj2018.04.0084, 2018.
- 517 Nixon, J.: Discrete ice lens theory for frost heave in soils, *Can Geotech J*, 28, 843-859, 10.1139/t91-102,
- 518 1991.
- 519 Oswald, S., Kinzelbach, W., Greiner, A., and Brix, G.: Observation of flow and transport processes in
- 520 artificial porous media via magnetic resonance imaging in three dimensions, *Geoderma*, 80, 417-429,
- 521 10.1016/S0016-7061(97)00064-5, 1997.
- 522 Oztas, T., and Fayetorbay, F.: Effect of freezing and thawing processes on soil aggregate stability, *Catena*,
- 523 52, 1-8, 10.1016/S0341-8162(02)00177-7, 2003.
- 524 Peng, X., Frauenfeld, O. W., Cao, B., Wang, K., Wang, H., Su, H., Huang, Z., Yue, D., and Zhang, T.:
- 525 Response of changes in seasonal soil freeze/thaw state to climate change from 1950 to 2010 across china,
- 526 *Journal of Geophysical Research Earth Surface*, 10.1002/2016JF003876, 2016.
- 527 Pittman, F., Mohammed, A., and Cey, E.: Effects of antecedent moisture and macroporosity on infiltration
- 528 and water flow in frozen soil, *Hydrol Process*, 34, 795-809, 10.1002/hyp.13629, 2020.
- 529 Smith, M.: Observations of soil freezing and frost heave at Inuvik, Northwest Territories, Canada, *Can J*
- 530 *Earth Sci*, 22, 283-290, 10.1016/0148-9062(85)90073-7, 1985.
- 531 Spaans, E. J.: The soil freezing characteristic: Its measurement and similarity to the soil moisture
- 532 characteristic, 1994.
- 533 Spaans, E. J., and Baker, J. M.: The soil freezing characteristic: Its measurement and similarity to the soil
- 534 moisture characteristic, *Soil Sci Soc Am J*, 60, 13-19, 10.2136/sssaj1996.03615995006000010005x, 1996.
- 535 Stadler, D., Stähli, M., Aeby, P., and Flüeler, H.: Dye tracing and image analysis for quantifying water
- 536 infiltration into frozen soils, *Soil Sci Soc Am J*, 64, 505-516, 10.2136/sssaj2000.642505x, 2000.
- 537 Stähli, M., Bayard, D., Wydler, H., and Flüeler, H.: Snowmelt Infiltration into Alpine Soils Visualized by



- 538 Dye Tracer Technique, *Arctic Antarctic & Alpine Research*, 36, 128-135, 10.1657/1523-
539 0430(2004)036[0128:SIASV]2.0.CO;2, 2004.
- 540 Taina, I. A., Heck, R. J., Deen, W., and Ma, E. Y.: Quantification of freeze–thaw related structure in
541 cultivated topsoils using X-ray computer tomography, *Can J Soil Sci*, 93, 533-553, 10.4141/CJSS2012-044,
542 2013.
- 543 Tarnawski, V. R., and Wagner, B.: On the prediction of hydraulic conductivity of frozen soils, *Can Geotech*
544 *J*, 33, 176-180, 10.1139/t96-033, 1996.
- 545 Wang, D., Yates, S., and Ernst, F.: Determining soil hydraulic properties using tension infiltrometers, time
546 domain reflectometry, and tensiometers, *Soil Sci Soc Am J*, 62, 318-325,
547 10.2136/sssaj1998.03615995006200020004x 1998.
- 548 Wang, X., Chen, R., Liu, G., Yang, Y., Song, Y., Liu, J., Liu, Z., Han, C., Liu, X., Guo, S., Wang, L., and
549 Zheng, Q.: Spatial distributions and temporal variations of the near-surface soil freeze state across China under
550 climate change, *Global Planet Change*, 172, 150-158, 10.1016/j.gloplacha.2018.09.016, 2019.
- 551 Watanabe, K., and Flury, M.: Capillary bundle model of hydraulic conductivity for frozen soil, *Water*
552 *Resour Res*, 44, 10.1029/2008WR007012, 2008.
- 553 Watanabe, K., and Wake, T.: Hydraulic conductivity in frozen unsaturated soil, *Proceedings of the 9th*
554 *International Conference on Permafrost*, 2008, 1927-1932,
- 555 Watanabe, K., Kito, T., Dun, S., Wu, J. Q., Greer, R. C., and Flury, M.: Water infiltration into a frozen soil
556 with simultaneous melting of the frozen layer, *Vadose Zone J*, 12, vzj2011.0188, 10.2136/vzj2011.0188, 2013.
- 557 Watanabe, K., and Kugisaki, Y.: Effect of macropores on soil freezing and thawing with infiltration, *Hydrol*
558 *Process*, 31, 270-278, 10.1002/hyp.10939, 2017.
- 559 Watanabe, K., and Osada, Y.: Simultaneous measurement of unfrozen water content and hydraulic



- 560 conductivity of partially frozen soil near 0 C, Cold Reg. Sci. Technol, 142, 79-84,
561 10.1016/j.coldregions.2017.08.002, 2017.
- 562 Watson, K., and Luxmoore, R.: Estimating macroporosity in a forest watershed by use of a tension
563 infiltrometer, Soil Sci Soc Am J, 50, 578-582, 10.2136/sssaj1986.03615995005000030007x, 1986.
- 564 Williams, P., and Burt, T.: Measurement of hydraulic conductivity of frozen soils, Can Geotech J, 11, 647-
565 650, 10.1139/t74-066, 1974.
- 566 Williams, P. J., and Smith, M. W.: The frozen earth: fundamentals of geocryology, Cambridge University
567 Press, 1989.
- 568 Wilson, G., and Luxmoore, R.: Infiltration, macroporosity, and mesoporosity distributions on two forested
569 watersheds, Soil Sci Soc Am J, 52, 329-335, 10.2136/sssaj1988.03615995005200020005x, 1988.
- 570 Wooding, R.: Steady infiltration from a shallow circular pond, Water Resour Res, 4, 1259-1273,
571 10.1029/WR004i006p01259, 1968.
- 572 Zhao, Y., Nishimura, T., Hill, R., and Miyazaki, T.: Determining hydraulic conductivity for air - filled
573 porosity in an unsaturated frozen soil by the multistep outflow method, Vadose Zone J, 12, 1-10,
574 10.2136/vzj2012.0061, 2013.